International Journal of Computer Information Systems and Industrial Management Applications.
ISSN 2150-7988 Volume 15 (2023) pp. 418-428

Received: 10 Feb. 2023; Accepted: 27 May, 2023; Published: 23 June, 2023

DNN and RNN Models derived by PSO for Predicting COVID-19 and R_t under Control Measure

Rati Wongsathan[1] and Wutthichai Puangmanee[2]

[1] Department of Electrical Engineering, Faculty of Engineering and Technology, North-Chiang Mai University,
169 Chiang Mai-Hot Road, Hang Dong, Chiang Mai 50230, Thailand
rati@northcm.ac.th

[2] Department of Computer Engineering, Faculty of Engineering and Technology, North-Chiang Mai University,
169 Chiang Mai-Hot Road, Hang Dong, Chiang Mai 50230, Thailand
wutthichai@northcm.ac.th

Abstract*: The COVID-19 pandemic novel coronavirus disease, a supernova in human history, caused considerable suffering and death worldwide. Thailand has experienced five surges of infection, each with unique and complex nonlinear dynamics. Therefore, the epidemic size and emerging trends cannot be estimated accurately, resulting in ineffective outbreak control. This study is to implement an adaptive prediction model using deep neural networks (DNN) and recurrent neural networks (RNN) machine-learning technologies. The challenge of this study relates to the use of previously short-term predicted values to attain the convergence of future trends. Moreover, mathematical demography is utilized to estimate the time-varying effective reproduction number (R_t), a metric that assesses the efficacy of control measure, based on the projected values. To avoid loss of robustness and generalization caused by the overfitted model, the optimal hyperparameters are derived using particle swarm optimization (PSO). To reduce the complexity, the dropout regularization technique is modified and applied to the DNN. Due to a lack of training data resulting in an under-fitted model problem, the outbreak data affected by COVID-19 virus mutations in countries that have surpassed the maximum point of infection before Thailand are encompassed in the training dataset, with their basic reproduction number ranges covering that of Thailand. After implementing the proposed models to Thailand's COVID-19 time series for the first through fifth surges, the simulation results show that the RNN-PSO model outperforms the others in terms of a considerably accurate estimation of the final epidemic size and lower RMSE, higher reliability, and higher R^2 for a developing epidemic trend. In addition, the estimated R_t from the RNN-PSO are consistent with the measures, reflecting the performance of the lockdown and vaccination measures under the viral mutants of each surge. This model can be applied to the upcoming surges and future epidemics and used in other areas.

***Keywords*:** COVID-19, reproduction number, deep neural network (DNN), recurrent neural network (RNN), dropout regularization, particle swarm optimization (PSO).

I. Introduction

Thailand, along with other countries, is currently facing the havoc of the COVID-19 pandemic. Until now (2022), there existed five surges of outbreaks in this country. Despite the vaccines and treatments available, the pandemic's end remains unknown**.** Authorities are continuously attempting to reduce the rate of viral spread by using various measures. In addition, predictions of the developing trend of the outbreak help decision-makers plan their responses to ongoing and future infection surges. Recently, academics have launched various techniques to model the transmission of viruses. These epidemiology models have developed from mathematical models [1]-[2] to statistical models [3]-[4], and, lately, to emerging machine learning (ML), such as logistic regression (LGR) [5], multilayer perceptron (MLP) [6], various neural networks (NN) [7]-[12], and others [13]-[14].

However, the trajectory of COVID-19 exhibits non-linear patterns that are subject to variations influenced by multiple factors, including cluster explosions, the effectiveness of control measures, and the emergence of viral mutations. These trends develop or deteriorate over time, making COVID-19 a time-series data in which future values depend on previous occurrences. Therefore, characterizing these dynamics requires an adaptive and robust model. To this end, the lack of memory units for capturing significant past data limits the predictions of mathematical models. Besides, the inability to track the fluctuations of an epidemic nature is a drawback of statistical models, which instead perform smooth average trends. Whereas the ML-based model has been demonstrated to be the most effective in characterizing COVID-19 time series, especially the NN models.

The application of NN to predict the incidence of COVID-19 ranges from shallow NN (SNN) [8] to deep NN (DNN) and recurrent NN (RNN) [9]-[11]. However, SNN has no memory units to keep up with past information, which may not be able to capture the dynamics of the epidemic, even well-training. This can be improved by inserting more hidden layers, i.e., DNN. Unlike RNN, the memory-based model with loops of feedback connections has proven to be better for predicting nonlinear and dynamic time series than others [12].

However, NN requires an extended training period to effectively capture and analyze the ongoing trends, thereby potentially impeding their applicability for timely planning objectives. Additionally, the absence of comprehensive COVID-19 outbreak data during the initial phases of infection presents constraints on the training process of NN models. To

address this problem, the previous study [15] employed alternative outbreak datasets, including those related to prior outbreaks such as MERS in 2012 and SARS in 2003, for training purposes. However, COVID-19 and these epidemics differ in terms of infection, and the data are outdated; thus, the model may be unreliable. Besides, most NN-based prediction models do not account for the temporal dependencies within the COVID-19 time series, which compromise the accuracy of the models. In [8], predictors with a 14-time lag, consistent with the incubation period of COVID-19 infection, are used as the input of the NN. However, this high input dimension may result in a correlation between them. Besides, the hyperparameters that improve learning and indirectly reduce complexity do not rely on analytical methods. Typically, they are adjusted iteratively using a trial-and-error approach, which may not result in achieving the optimal performance.

In this research, a prediction model is implemented utilizing DNN and RNN to estimate the final size of the epidemic and the trajectory of the first to fifth surges of COVID-19 in Thailand. To ensure the applicability of the models during the early phase, short-term forecasting of cumulative cases is conducted with a one-week-ahead prediction, considering the limited availability of COVID-19 data. The predicted values of previous surges are incorporated into the predictor set to estimate the subsequent values, and this process is repeated until convergence, allowing for the forecasting of the future trends in each surge. Moreover, by mathematical demography, the time-varying effective reproduction number (R_t), which captures the disease's spread dynamics while accounting for control measures, is estimated using these projected values. To enhance the training of the DNN and RNN models, the training dataset incorporates data from other countries that have experienced the maximum point of infection, including instances involving viral mutants. Furthermore, the particle swarm optimization (PSO), known for its simplicity, speed, and efficiency, is employed to determine the optimal hyperparameters, including the input time-lag, to mitigate model complexity [16]-[17]. Moreover, the implementation of dropout regularization technique is utilized to mitigate the VGP while simultaneously reducing the learning complexity. The performance of the proposed models is compared with that of SNN and previous studies to evaluate their predictive capability.

II. Methods

A. Data

The collection of secondary data on active COVID-19 cases in Thailand involves sourcing information from Ministry of Public Health, Thailand, while data pertaining to other countries are obtained from the Worldometer website and WHO. The dataset in this study is carefully selected to construct the data and the range of reproduction numbers, covering those observed in Thailand. Maximum and minimum values outside the data range are determined to support the predicted data and are used to normalize the data to remove different scales among the predictors.

B. Prediction Models

The COVID-19 case prediction as a function of the current (S_t) and past values (S_{t-1}, S_{t-2}, …, S_{t-N}), where N is the maximum time lag, can be mathematically expressed as,

$$\hat{S}_{t+1:t+m} = f_{nl}([S_t, S_{t-1}, ..., S_{t-N}]^{\mathrm{T}}) + \varepsilon\,, \tag{1}$$

where $m = 1, 2, \ldots, M < N$, f_{nl} is a nonlinear transformation function, and ε denotes prediction errors.

To make short-term predictions, i.e., $M \le 7$. Utilizing the estimated remaining trend and final epidemic size, the predicted values are reintegrated into the predictor set to forecast the subsequent M days (Figure 1). This process is repeated until the final size of the epidemic converges. To overcome error propagation, the predicted values are stored in the tracking list while checking them with the available actual data at the beginning of the outbreak. The prediction models based on the DNN and RNN are detailed in the following Sub-sections.

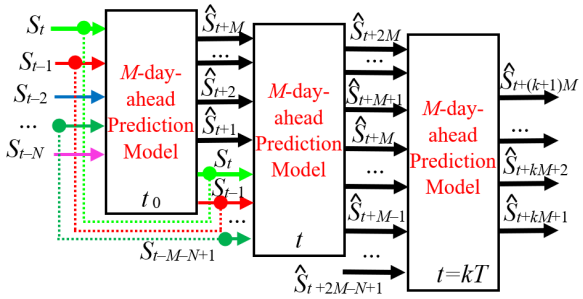

Figure 1. Short-term prediction involves forecasting the M-horizon and constructing a new predictor set with an N-input by utilizing the previously predicted values to estimate consecutive values.

1) DNN-based Prediction Model

The study reveals that the SNN model, consisting of a limited number of hidden layers, can effectively serve as a prediction model for COVID-19 solely in countries that have encountered the initial maximum point of infection [7]-[8], which is a limitation. To overcome this problem, a deep NN (DNN) is an alternative model, which has many hidden layers and nodes (Figure 2).

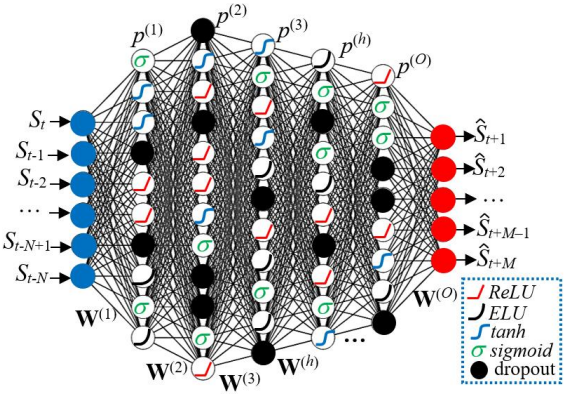

Figure 2. Structure of the DNN-based prediction model with dropout technique for predicting M-day-ahead COVID-19 cases using current and N-lag of past samples.

However, the vanishing gradient problem (VGP) is a prominent issue encountered in DNNs, wherein the error gradient propagated from the output to adjust the connected weights diminishes gradually. To address this challenge, a set of activation functions, including the rectified linear unit (ReLU(x) = max[0, x]) and exponential linear unit (ELU(x) =

max[ae^x–1, x]), where $a \in R^+$, are incorporated alongside conventional squashing functions (i.e., $\nabla e(x) \neq 0$, for $x > 0$) like the hyperbolic tangent (*tanh*) and sigmoid (σ). This integration of activation functions, denotes as $\psi = \{tanh, \sigma, ReLU, ELU\}$, aims to overcome the VGP in DNNs.

In addition, the overfitting problem due to a small number of training data memorized by a number of DNN parameters causes loss of generalization, i.e., failure in predicting when met the unseen input data. In this study, the dropout method [18], a regularization technique that removes the redundant hidden nodes in each hidden layer is employed to improve the learning with the BPA, while reducing the DNN complexity. Generally, the dropout DNN is applied only to the training phase in the classification problem. However, this gives an average output. In the prediction requiring the precision value, it is enabled in the test phase. Furthermore, the dropout actives for only some of the first training epochs for accelerating the learning, and the BPA takes for the remaining epochs. Using the dropout technique, the hidden nodes in the NN are temporarily deactivated with a dropout ratio 1– $p^{(l)}$, where l represents the specific hidden layer (ranging from 1 to L, the maximum hidden layer). This can be observed in Figure 2, where the deactivated nodes are depicted in black. It is worth mentioning that the dropout rate, denoted as p, is expressed using the Python language in Keras, a deep learning library. Therefore, 2^{HN}-thicken DNNs are generated, where $HN=M\times(\Pi H^{(l)})\times N$ and $H^{(l)}$ is the number of hidden nodes in l^{th}-hidden layer. The dropout DNN-based prediction can be expressed as,

$$\hat{S}_{DNN}(t+m) = \psi^{(o)} \sum_{j=1}^{H^{(L)}} \frac{\mathbf{D}^{(l)}}{1-p^{(l)}} \phi, \tag{2}$$

where

$$\phi = \psi_j^{(L)} \sum_{k=1}^{H^{(L-1)}} w_{j,k}^{(L)} \left(\cdots \psi_i^{(1)} \left(\sum_{l=0}^{N} w_{i,l}^{(1)} S(t-l) \right) \right), \tag{3}$$

and $\mathbf{D}^{(l)} : D_n^{(l)} \sim Bernoulli(p^{(l)})$, n = 1,2, …, $H^{(l)}$.

The BPA involves training the dropout DNN using a specific criterion, expressed as:

$$Min\, J = \sum_i \left\| S_{t+i}^{Actual} - \hat{S}_{t+i} \right\|. \tag{4}$$

The connected weights, including the biases, of the dropout DNN are iteratively updated at the $iter^{\text{th}}$-iteration using Equation (5), with the learning rated denoted as η.

$$\mathbf{W}_{iter}^{(l)} \leftarrow \mathbf{W}_{iter}^{(l)} + \eta \mathbf{D}^{(l)} \frac{\partial J}{\partial \mathbf{W}^{(l)}}. \tag{5}$$

2) ERNN-based Prediction Model

Typically, SNN or DNN cannot capture past information from a time series. They only learn a nonlinear relationship between current inputs and outputs. Alternatively, RNNs with built-in memory can learn a dynamic nonlinear relationship. Elman RNN (ERNN) among them has been proven to be more effective in prediction than others in many fields [19]. The M-element prediction output vector ($\hat{\mathbf{S}}$) of the ERNN (Figure 3) with a single hidden layer and connections from H hidden nodes to context units in the matrix form are as follows,

$$\hat{\mathbf{S}} \equiv [S_{t+1}, ..., S_{t+M}]^{\mathrm{T}} = \mathbf{W}_O \left(f_{tanh}(\mathbf{W}_S \mathbf{S}_t + \mathbf{W}_C \mathbf{C}_t) \right), \tag{6}$$

$$\mathbf{C}_{t+1} = f_{tanh}(\mathbf{W}_S \mathbf{S}_t + \mathbf{W}_C \mathbf{C}_t), \quad \mathbf{C}(\underline{\mathbf{0}}) = 0, \tag{7}$$

where $\mathbf{S}_t$ and $\mathbf{C}_t$ represent the N-element predictor vector and the H-element context node vector, respectively, and f_{tanh} denotes tangent hyperbolic function. The weight matrices, denoted as $\mathbf{W}_S$, $\mathbf{W}_C$, and $\mathbf{W}_O$, establish connections between the input-to-hidden layer, hidden-to-context layer, and hidden-to-output layer, respectively.

In training the ERNN using BPA, the errors are fed back to update the $\mathbf{W}_O$, $\mathbf{W}_S$, and $\mathbf{W}_C$ under the criterion of Equation (4), as follows,

$$\mathbf{W}_O \leftarrow \mathbf{W}_O + \alpha \cdot \mathbf{H}_O \cdot \nabla \mathbf{e}, \tag{8}$$

$$\mathbf{W}_S \leftarrow \mathbf{W}_S + \eta \cdot (\nabla \mathbf{H}_O) \cdot (\nabla \mathbf{e}) \cdot \mathbf{S}_t, \tag{9}$$

$$\mathbf{W}_C \leftarrow \mathbf{W}_C + \alpha \cdot (\nabla \mathbf{H}_O) \cdot (\nabla \mathbf{e}) \cdot \mathbf{C}_t. \tag{10}$$

However, RNNs like other NNs experience over-fitting through the learning process. To overcome this problem, a validation-based early stopping technique terminates the training process when the convergence of the MSE criterion is started.

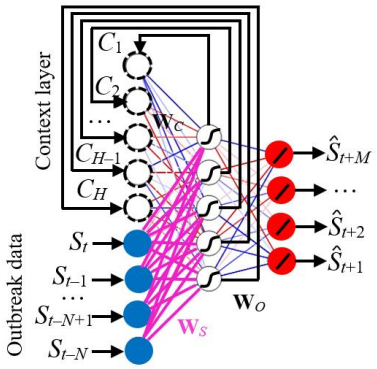

Figure 3. Structure of the ERNN-based COVID-19 prediction model for predicting M-day-ahead infected cases using current and N-lag of past samples.

3) Optimization of the Hyperparameters

The optimal time lag (N), hidden layer (L), hidden node each layer l ($H^{(l)}$), and prediction length (M) could not be determined analytically. A higher N means a large amount of training data is required, increasing the likelihood of overfitting. On the other hand, an increased prediction length leads to more accumulated errors. Moreover, the increase in L and $H^{(l)}$ results in complexity and many NN parameters, leading to VGP and local trap problem in training. As a COVID-19 time series related to the number of infections

with a trendy *S*-shaped like without noise due to the accurate measurement, a simple NN structure with a few hidden layers, each of which requires a moderate number of hidden nodes, is sufficient to model these series.

The hyperparameters; N, L, M, and $H^{(l)}$, including ψ, p, η, and the number of epochs (*epoch*), are optimized to improve the performance of the DNN and ERNN models. A total of $2L+19$ dimensions are considered for DNN hyperparameters, incorporating L hidden nodes within each hidden layer, four function combinations (2^4-1)–ψ, L dropout ratios for each hidden layer, and four parameters associated with N, M, η, and *epoch*. On the other hand, the single hidden layer ERNN hyperparameters without dropout only have 19 dimensions that are optimized. However, the large dimensions of the search, especially for DNN with varying L, require a simple and effective optimization approach. In this study, PSO, a bio-inspired swarm intelligence, is utilized due to its simplicity and minimal parameter requirements.

In the PSO procedure (Figure 4), each of N_p-particle possesses a position vector ($\mathbf{X}_q$) of either $2L+19$ or 19 elements for dropout DNN and ERNN, respectively, where $q=1, \ldots, N_p$. Each particle moves according to its velocity vector ($\mathbf{V}_q$). At i^{th}-iteration, the q^{th}-particle moves with velocity v_q from Location 1 to 2 along the yellow line. The fitness of all particles is evaluated using the fitness function J (11). The personal best vector, $\mathbf{P}_{best}(i)$, and the global best, $\mathbf{G}_{best}$, are updated as follows: $P_{best,q}(i)=P_q(i)$ if $P_q(i) > P_{best,q}(i-1)$, and $G_{best}(i) = P_{best,q}(i)$ if $P_q(i) > G_{best}(i)$, where $i = 1, \ldots, iter_{max}$ (maximum iteration).

$$J(\mathbf{X}_q(i)) = \sum_j^{N_T-N+1} \lambda^{M-N_T+1-i} \left\| \mathbf{S}-\mathbf{S} \right\|_j , \tag{11}$$

where N_T represents the total number of training data.

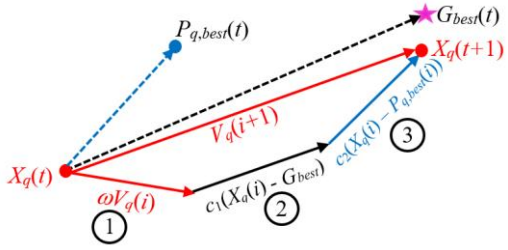

Figure 4. Diagram of PSO-based selection optimal hyperparameters for DNN and ERNN.

The particles connect to each other to obtain information for making decisions to move toward the resultant direction influenced by both their local best position ($P_{best,q}$) and the global best position (G_{best}) from Location 2 to 3. Their new velocities and position vectors are as follows,

$$\begin{aligned} V_q(i+1) = \omega V_q(i) + c_1(X_q - P_{best,q})(i) \\ + c_2(X_q - G_{best})(i) \end{aligned} , \tag{12}$$

$$\mathbf{X}_q(i+1) = \mathbf{X}_q(i) + \mathbf{V}_q(i+1) , \tag{13}$$

respectively, here ω denotes the inertia weight with typically assigning to less than 1, and c_1 and c_2 represent acceleration constants chosen from the range of [1, 3]. Throughout the procedure, these values are pre-determined and fixed. The optimization process continues until the stopping criteria are met. The pseudocode of PSO for the hyperparameters of DNN and ERNN is shown in Figure 5.

Pseudocode: Optimal hyperparameters of the proposed dropout DNN and ERNN using PSO for predicting COVID-19 cases.

Input: $\{L, N^{(l)}, \psi, N, M, p, \eta, \lambda, epoch\}$
Training input: $S(t), \ldots, S(t\text{-}N)$
$epoch$ =1
While $epoch < epoch_{max}$
Initialization: N_p, $\mathbf{X}q(0)$, $\mathbf{V}q(0)$, $P_{best,q}(0)$,
While $i < iter_{max}$ (Maximum iteration)
Training DNN/ERNN by BPA to minimize J Eq. (4)
Update the weights and biases using Eq. (5), and Eq.(8)-(10)
Evaluating q^{th}-particle: argmin $J_{pso}(X_q(i))$
$G_{best}(i)$=arg min $f(P_{best,q}(i))$
Update V_q Eq. (12) and $\mathbf{X}_q$ Eq. (13)
If $f_{pso}(X_q(i)) < f_{pso}(P_{best,q}(i)) \rightarrow P_{best,q}(i) = X_q(i)$
If $f_{pso}(X_q(i)) < f_{pso}(G_{best}(i)) \rightarrow G_{best}(i) = X_q(i)$
End (While)
epoch←epoch+1
End (While)
Output: Optimal dropout DNN and ERNN

Figure 5. Pseudocode of hyperparameter selection using PSO and training DNN and ERNN.

4) Estimation of Reproduction Number

The basic reproduction number (R_0), as well as effective reproduction number ($R(t)$), serves as metrics for quantifying the average number of new infections emerging from an individual infected. They are used to indicate the strength of epidemic transmission and assess the effectiveness of the control measures. Various methods can be used to estimate $R(t)$. In this study, it can be estimated using the predicted cumulative cases obtained from the DNN or ERNN models through mathematical demography [20],

$$R(t-t_0) = \frac{\overset{次}{S}(t) - S(t-1)}{\sum_{a=u}^{a=v} W(a)\left(\overset{次}{S}(t-t_0) - S(t-1)\right)} \tag{14}$$

where

$$W(a) = ge^{-ga} \big/ (e^{-gu} - e^{-gv}) , \tag{15}$$

represents the distribution of the survival function for the infectious state, which denotes the proportion of individuals that remain contagious (t–a) days after infection. In this equation, t_0 represents the lag in days between the infection date and the reported cases, g represents the recovery rate, and [u, v] denotes the duration of infection. To simulate $R(t)$, g = 0.1, as recommended by the WHO (2020) is utilized, which may be changed in the future.

5) Optimization of the Hyperparameters

Two widely used metrics evaluate the model accuracy and the fit-to-model including root mean square error (RMSE) and coefficient of determination (R^2). The RMSE measures the average magnitude of the prediction errors, with lower values indicating better model performance. On the other hand, R^2 quantifies the proportion of the variance in the observed data that can be explained by the model, with higher values indicating a better fit.

$$RMSE = \sqrt{\frac{1}{N}\sum_i (S_i - \hat{S}_i)^2}\,, \tag{16}$$

$$R^2 = \frac{\sum_i (\hat{S}_i - \bar{S}_i)^2}{\sum_i (S_i - \bar{S}_i)^2}, \tag{17}$$

where $\bar{S}$ represents the mean of the measured data.

In addition to the model's accuracy, the reliability of the predictions model is crucial. Among the reliability tests, the test-retest reliability, the degree to which the predicted results are consistent over a period when using the same dataset in training the model, is the most used. It can be measured by test-retest correlation of the Pearson correlation coefficient,

$$\rho = \frac{\sum_i (\hat{S}_{1,i} - \bar{S}_{1,i}) - (\sum_i S_{2,i} - \bar{S}_{2,i})}{\sqrt{\sum_i (\hat{S}_{1,i} - \bar{S}_{1,i})^2 \sum_i (S_{2,i} - \bar{S}_{2,i})}}\,, \tag{18}$$

where $\hat{S}_{1,i}$, $\hat{S}_{2,i}$ and $\bar{S}_{1,i}$, $\bar{S}_{2,i}$ represents the predicted results of the test and retest, and the mean values of them, respectively.

In the prediction task using the NN model with different predicted results each time due to the initial values of weights and biases used in the BPA training, Equation (18) can be repeated and then averaged. Typically, the range classifications for ρ-values are as follows: [0-0.4) signifies low correlation, [0.4, 0.70) denotes moderate correlation, [0.7, 0.9) suggests high correlation, and [0.9, 1] indicates very high correlation.

Since each surge of infection in Thailand is different due to the type of viral mutant, control measures actioned during the outbreak, and other exogenous factors, different prediction models are formulated based on these five surges of infection.

III. Results and Discussion

The optimal hyperparameters set, $\theta = \{N, M, L, H^{(l)}, \psi, p, \eta, epoch\}$ and $\theta = \{N, M, H, \psi, \eta, epoch\}$, required to enhance the performance of the DNN and ERNN are selected among the combinations shown in Table 1 and Table 2, respectively.

A. The first surge of Thailand's COVID-19 (January – May 2020)

In the initial phases of the first surge of infection, there is a lack of sufficient outbreak data to train the NNs. To address this limitation, outbreak data from other countries that have already surpassed the maximum point of infection are included in the training process, along with a few samples from the early stages in Thailand. The basic reproduction number (R_0) of these countries should range, covering that of Thailand. Therefore, the training data taken from countries, including China, India, Hong Kong, and South Korea, whose cumulative cases with their R_0 values against those of Thailand are considered (Figure 5). To preliminarily check the similarity of the data, the cross-correlation indices (ρ) with offset time lags between the time series data of the countries and those of Thailand are about 0.8717 (0-lag) for China, 0.6922 (48-lag) for Hong Kong, 0.7487 (24-lag) for Korea, and 0.6105 (25-lag) for India, respectively. Therefore, the outbreak data of China and Korea, which have high similarities to Thailand, are included in the predictor set. It is seen that the MSE performance during training increases when using these outbreak data (Figure 6). In addition, a low variance of MSE in several experiments indicates the robustness and generalization to unseen data of the model. For the ERNN-PSO model with these outbreak data in the training and testing phases, the accuracy of the final epidemic size and future trends are significantly improved (Figure 7).

θ	Range	Surge1	Surge2	Surge3	Surge4	Surge5
N	[2, 20]	7	5	5	6	5
M	[1, 7]	2	2	3	3	1
L	[2, 10]	5	7	5	5	5
$H^{(l)}$	[10, 100]	20,25, 39,28, 22	30,28, 30,25, 13,30, 11	28, 30, 22, 25, 20	25,30, 23,22, 20	33,20, 28,25, 17
ψ	{ReLU, ELU, tanh, σ}	{ReLU, tanh, σ}	{ELU, ReLU, tanh σ}	{ReLU, tanh, σ}	{ELU, tanh, σ}	{ReLU, tanh, σ}
p	[0.1, 0.5]	0.12, 0.17, 0.20, 0.15, 0.31	0.15, 0.27, 0.19, 0.15, 0.33, 0.21, 0.18	0.21 0.27, 0.18, 0.25, 0.07	0.19, 0.27, 0.25, 0.13, 0.31	0.13, 0.23, 0.19, 0.45, 0.19
η	[10^{-3},0.1]	0.0012	0.0013	0.0015	0.0013	0.0028
epoch	[500,10^4]	7,000	12,000	9,500	9,500	7,500

Table 1. Selecting optimal hyperparameters of the DNN-based COVID-19 prediction model using PSO.

θ	Range	Surge1	Surge2	Surge3	Surge4	Surge5
N	[2, 20]	9	12	10	8	7
M	[1, 7]	3	2	4	3	3
H	[10, 150]	80	130	50	60	50
ψ	{ReLU, ELU, tanh, σ}	{ReLU, tanh, σ}	{ELU, tanh, σ}	{ReLU, ELU, tanh}	{ReLU, tanh, σ}	{ReLU, ELU, σ}
η	[10^{-3},0.1]	0.0012	0.0015	0.0028	0.0019	0.0023
epoch	[500,10^4]	6,500	10,000	7,000	7,500	6,500

Table 2. Selecting optimal hyperparameters of the ERNN-based COVID-19 prediction model using PSO.

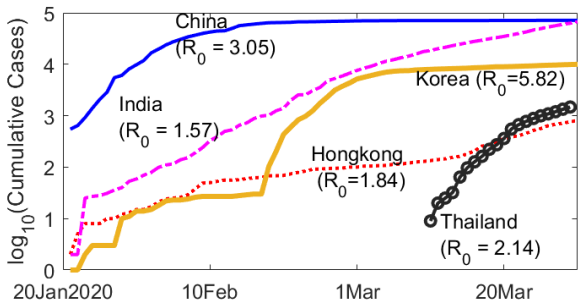

Figure 5. Developing trends and basic reproduction number (R_0) of Thailand's first surge of COVID-19 against China, Hong Kong, South Korea, and India.

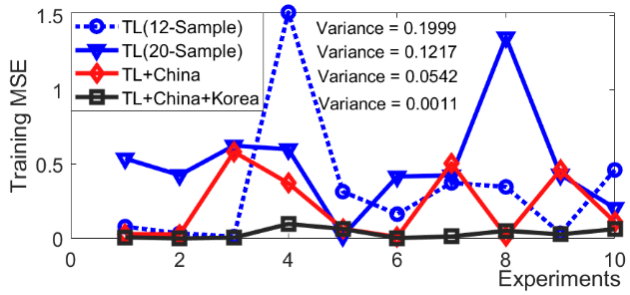

Figure 6. MSEs and their variance during the training phase of the epidemic ERNN with different predictor sets, including outbreak data from China and Korea, for modeling Thailand's first surge of the COVID-19 epidemic.

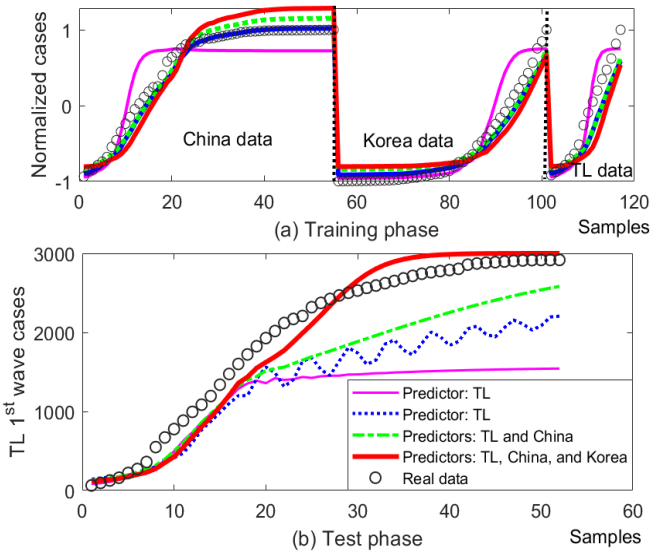

Figure 7. Prediction results of the ERNN-PSO model using different predictor sets in (a) training and (b) test phases for Thailand's first surge of the COVID-19 epidemic.

Figure 8 depicts the prediction results among the NN models and the logistic growth regression model tunning by genetic algorithm (LGR/GA) and the logistic model in previous studies [5, 18] for Thailand's first COVID-19 surge.

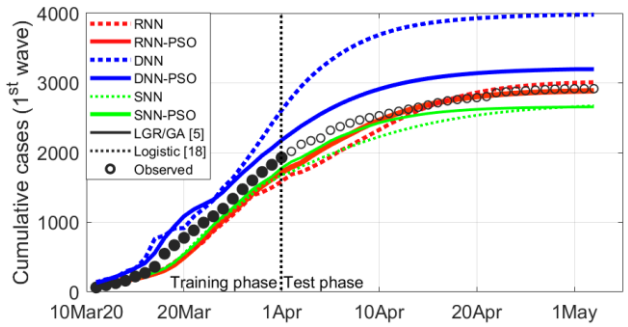

Figure 8. Prediction results of cumulative cases from the proposed models using outbreak data from China and Korea in training against the LGR/GA model [5] and the logistic model [21] for Thailand's first surge of COVID-19 epidemic.

Table 3 presents the performance indices of the prediction models. The proposed RNN-PSO outperforms the others in terms of high estimated epidemic final size, low RMSE of the developing trend, high reliability with a higher correlation coefficient, and a high-fit model with a higher R^2-value. Whereas the DNN and DNN-PSO models overestimate the epidemic trend, resulting in very high RMSE. In addition, the estimated R_t evaluated using the predicted values obtained from the ERNN-PSO are consistent with the measured values when compared to those of the rest. The decline in R_t to zero over time implies the effectiveness of the combination of lockdown and curfew measures taken after the super spread during the first surge of infection. This prevents hospital overload and results in the lack of medical staff. However, this affects social life and economics.

Model	Final epidemic size		Developing trends		
	Forecast	Error*	RMSE	ρ	R^2
ERNN-PSO	2910	7	183.7	0.995	0.983
ERNN	3001	84	207.0	0.988	0.976
DNN-PSO	3196	279	2012.9	0.986	0.977
DNN	3978	1061	5005.7	0.972	0.954
SNN-PSO	2607	310	253.9	0.993	0.929
SNN	2607	310	265.5	0.991	0.927
LGR/GA [5]	2532	385	332.7	0.827	0.873
Logistic [21]	2298	619	457.3	0.836	0.732

Table 3. Comparative analysis of prediction models for Thailand's first surge of COVID-19, with the actual final epidemic size recorded as 2,917*.

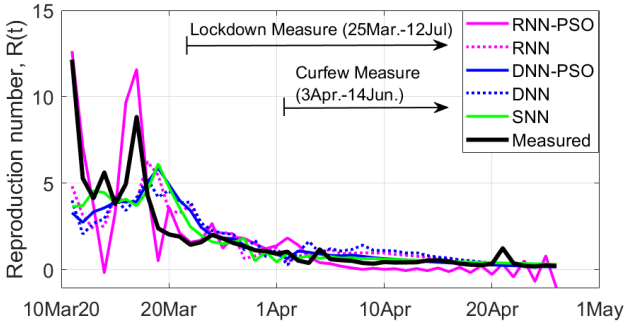

Figure 9. Reproduction number obtained from ERNN, DNN, and SNN with the measured data under curfew and lockdown measures for Thailand's first surge of COVID-19.

B. The Second surge of Thailand's COVID-19 with the Alpha variant (December 2020-February 2021)

After the first surge of infection ended, disease control measures were relaxed, resulting in cluster explosions, such as the "DJ cluster," which spread across the country after people became infected at a party in Bangkok, the capital. In addition, the alpha variant of COVID-19 began to spread throughout the country. As a result, the second surge of infection started with initial fluctuations in the trend of daily infected cases, causing the infection curve to have multiple maximum points of infection, deforming the conventional *S*-shaped cumulative case curve. These factors have made this surge complicated to predict and present a significant challenge. To address this problem, the predictor set includes outbreak data from countries that have passed the second surge of infection prior to Thailand, as well as the method used in the first surge of infection. Here, the outbreak data of China, Hong Kong, Korea, and India are included in the training dataset, along with those of the first surge and some at the beginning of the second surge in Thailand.

The cross-correlation indices (ρ) with offset time lags between the time-series data of China, Hong Kong, Korea, India, and Thailand's first surge and that of Thailand's second

surge are about 0.778 (-26-lag), 0.923 (11-lag), 0.908 (0-lag), 0.936 (0-lag), and 0.789 (-21-lag), respectively. In training experiments, the outbreak data after a shifted time lag from India, along with some of Thailand's second surge, are the best predictor set (Figure 10). The model learns well to capture sudden changes. Whereas, learning with the other predictor sets results in underestimated predictions and first peak traps.

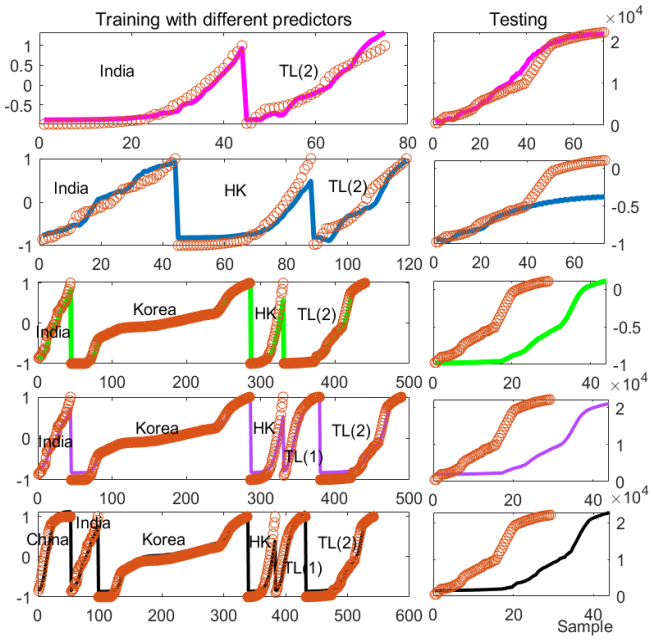

Figure 10. The performance of the ERNN in the training phase using different predictor sets, including outbreak data from China, India, Korea, Hong Kong, and Thailand's first surge, for Thailand's second surge of COVID-19 epidemic.

In the test comparison, the proposed ERNN-PSO outperforms the rest in terms of low estimated error for estimating the final epidemic size. Except for the DNNs, the rest underestimate the final epidemic size because the predictions are trapped in the first peak. The DNN-PSO performs very well in characterizing the trend during the beginning and middle of the outbreak, but explodes highly at the end, resulting in a high RMSE. The SNN exhibits a more oscillating trend. Moreover, the ERNN-PSO provides low RMSE, high reliability with a higher correlation coefficient, and a high-fit model reflected by a higher R^2-value, enabling effective characterization of the developing trends (refer to Figure 11 and Table 4).

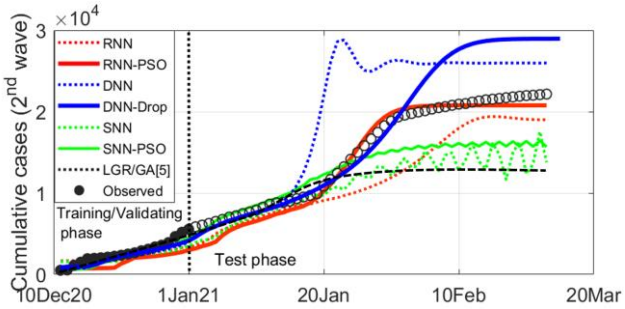

Figure 11. Prediction results of cumulative cases from the proposed models using the data outbreak from India in training against the LGR/GA model [5] for Thailand's second surge of COVID-19 epidemic.

Model	Final epidemic size		Developing trends		
	Forecast	Error*	RMSE	ρ	R^2
ERNN-PSO	2.078×10^4	1,381	183.7	0.995	0.989
ERNN	1.90×10^4	3,155	3,070	0.994	0.951
DNN-PSO	2.428×10^4	6,796	12,534	0.971	0.973
DNN	2.289×10^4	3,813	27,702	0.874	0.908
SNN-PSO	1.568×10^4	6,474	3,078	0.969	0.937
SNN	1.378×10^4	8,382	4,248	0.968	0.940
LGR/GA [9]	1.368×10^4	8,372	3,473	0.873	0.934

Table 4. Comparative analysis of prediction models for Thailand's second surge of COVID-19, with the actual final epidemic size recorded as 22,162*.

The estimated R_t values obtained from all prediction models differ significantly from the measured data because of the prediction errors for this surge (Figure 12). To address the problem, the interventions must incorporate into the predictor set. The measured R_t has multiple maximum points of infection due to many super-spreaders after the first surge is terminated with a loose strict measure. However, the implementation of a lockdown in vulnerable areas results in a rapid reduction of R_t indicating the effectiveness of this measure in containing the outbreak.

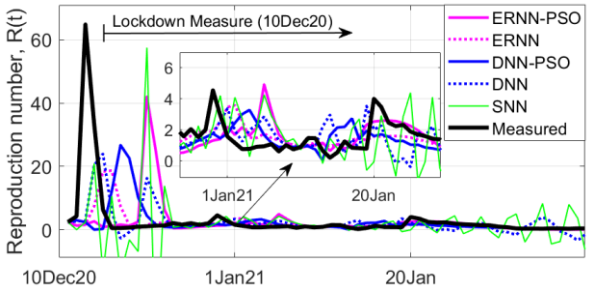

Figure 12. Reproduction number for Thailand's second surge of COVID-19 obtained from ERNN, DNN, and SNN models using measured data under lockdown measures.

C. The third surge of Thailand's COVID-19 (April – June 2021)

After the second surge, in April 2021 most of the COVID-19 infection in Thailand was the Alpha variant, whereas the situation abroad was the Delta variant, which began spreading in India. In May 2021, the number of cases in Thailand reached 100,000 for the first time. Many provinces have established additional field hospitals during state quarantine, but this does not seem sufficient. Lockdown measures are still in place, whereas vaccination is not widely distributed.

The Alpha variant was first detected in November 2020 in the UK. Also, it is the dominant variant in the USA. Therefore, the training dataset incorporates outbreak data from both countries, in addition to Thailand's previous two surges. The cross correlations between them from the UK, the USA, and the 1st and 2nd surges from Thailand and those at the beginning of Thailand's 3rd surge are approximately 0.943 (0-lag), 0.732 (33-lag), 0.693 (0-lag), and 0.967 (34-lag), respectively. During the training phase, all outbreak data exhibit the optimal predictor set (Figure 13). In the testing phase, the ERNN-PSO model outperforms the other models by exhibiting lower estimated errors in predicting the final epidemic size, lower RMSE values, higher reliability with a greater correlation coefficient, and better model fit with

higher R^2 values for capturing the evolving trends (Figure 14 and Table 5). However, this surge shows an incomplete cycle with a short right-hand-tail *S*-curve; therefore, the results cannot be confirmed without actual data.

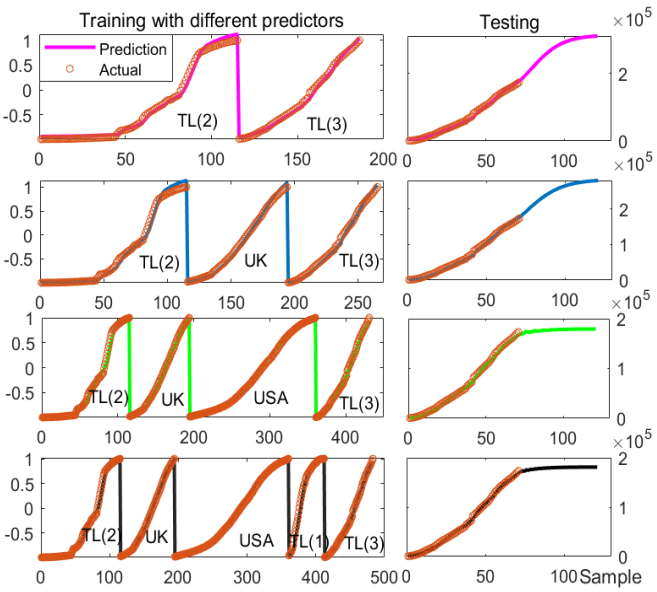

Figure 13. Performance of the ERNN in the training phase using different predictor sets, including data outbreaks from the UK, USA, and Thailand's previous two surges for Thailand's third surge of COVID-19.

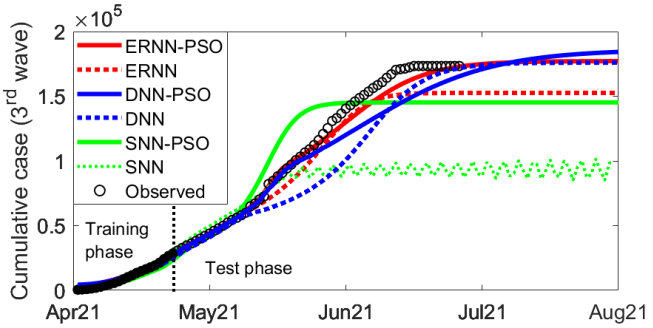

Figure 14. Prediction results of cumulative cases of the proposed models using data outbreaks from the UK, USA, and Thailand's previous two surges in training for Thailand's third surge of COVID-19 epidemic.

Model	Final epidemic size		Developing trends		
	Forecast	Error*	RMSE	ρ	R^2
ERNN-PSO	1.73×10^5	432	5.48×10^3	0.999	0.997
ERNN	1.525×10^5	2.07×10^4	1.08×10^4	0.962	0.997
DNN-PSO	1.654×10^5	1,643	6.59×10^4	0.977	0.993
DNN	1.717×10^5	7,918	1.19×10^5	0.940	0.983
SNN-PSO	1.45×10^4	2.81×10^4	1.71×10^4	0.838	0.925
SNN	1.08×10^4	1.62×10^5	8.75×10^5	0.758	0.735

Table 5. Comparative analysis of prediction models for Thailand's third surge of COVID-19, with the actual final epidemic size recorded as 173,349*.

The estimated R_t values obtained from all prediction models, especially for the ERNN-PSO, are consistent with the measured data (Figure 15). The R_t declines over the time due to the combination in vaccination and lockdown measures used in this surge. However, R_t remains nearly constant for a long time, reflecting the efficiency reduction of the lockdown measure with a large number of infected people.

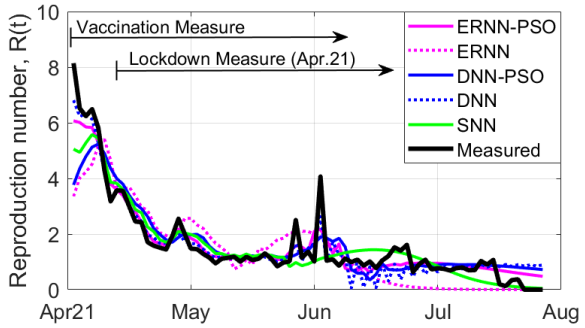

Figure 15. Reproduction number comparison among ERNN, DNN, and SNN models using measured data during the implementation of a lockdown measure for Thailand's third surge of COVID-19.

D. Fourth surge of Thailand's COVID-19 with the Delta variant (June 2020 – January 2021)

During the fourth surge of infection due to the delta variant, the number of COVID-19 cases in Thailand increased rapidly, making it difficult to control more than 100 cluster outbreaks. As of August 2021, the number of cases reached one million for the first time. Until now, we have had enough training data from the previous surges of infection. However, contrary to expectations, the prediction models perform well in the training phase but not in the prediction phase when using them (Figure 16). This supports the difference in the infection of virus mutants and the control measures of each surge.

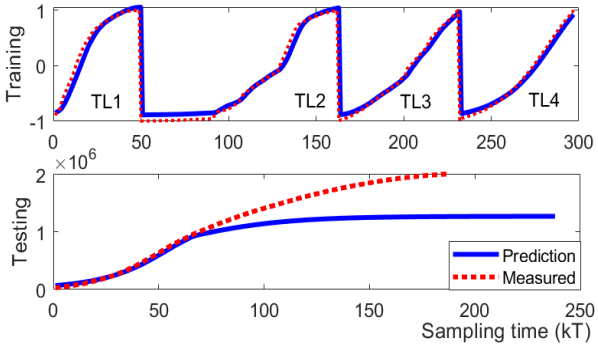

Figure 16. Training the ERNN model using the outbreak data set from the Thailand's past three surges for Thailand's fourth surge of COVID-19 epidemic.

Since the Delta variant was first detected in India in October 2020, it has exploded in February 2021 with massive deaths and spread to the UK, South Africa (SA), the USA, Australia (Aus.), and other countries. So, the outbreak data of countries that have highly similar patterns to those of the fourth surge of Thailand are included in the training dataset with those of the previous three surges. The cross-correlation coefficients between Thailand's fourth surge and the outbreaks in India, SA, Aus., and the UK were found to be approximately 0.919 (with a lag of 230 days), 0.904 (with a lag of 33 days), 0.889 (with a lag of 69 days), and 0.865 (with a lag of 149 days), respectively. In training, the outbreak data from all the countries mentioned above with a shifted time lag, as well as those from Thailand's previous three surges, are the best predictor set (Figure 17).

In the test, the ERNN-PSO forecasts the final epidemic size slightly less accurately than the DNN with oscillations and SNN-PSO with high rise-time, but it outperforms them, including the others, in terms of low RMSE and high reliability with a higher correlation coefficient and model-fit with higher R^2 to characterize the developing trends (Figure 18 and Table 6). However, this surge shows an incomplete cycle with a short right-hand-tail *S*-curve; therefore, the results cannot be confirmed without actual data.

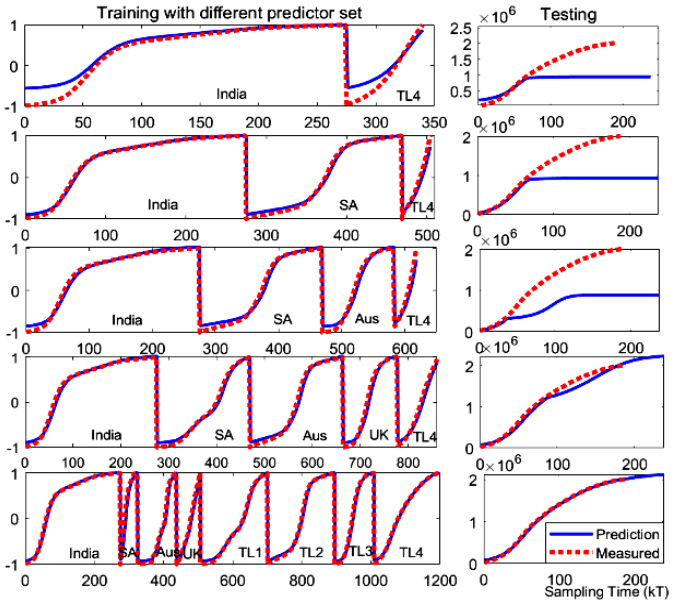

Figure 17. Performance of the ERNN-PSO in the training phase using different predictor sets in combination with the outbreak data from India, SA, Aus., the UK, and Thailand's past three surges for Thailand's fourth surge of the COVID-19 epidemic.

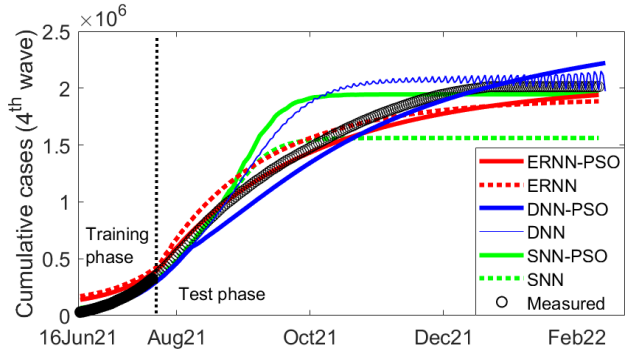

Figure 18. Prediction results of cumulative cases from the proposed models using the data outbreak India, SA, Aus., the UK, and Thailand's past three surges for Thailand's fourth surge of COVID-19 epidemic.

Model	Final epidemic size		Developing trends		
	Forecast	Error*	RMSE	ρ	R^2
RNN-PSO	1.946×10^6	7.20×10^4	1.05×10^5	0.999	0.997
RNN	1.884×10^6	1.28×10^5	1.27×10^5	0.992	0.985
DNN-PSO	2.21×10^6	3.03×10^4	7.50×10^5	0.970	0.963
DNN	1.98×10^6	1.86×10^6	3.14×10^5	0.958	0.903
SNN-PSO	1.94×10^6	6.72×10^4	1.95×10^5	0.943	0.937
SNN	1.562×10^6	4.51×10^5	2.74×10^5	0.919	0.921

Table 6. Comparative analysis of prediction models for Thailand's fourth surge of COVID-19, with the actual final epidemic size recorded as 2,012,738*.

The estimated $R(t)$ values obtained from the ERNN-PSO and ERNN models are consistent with the actual data (Figure 19). In this surge, the vaccination is initially taken without the lockdown measure, which are implemented for the previous three surges. So, partial immunity does not completely reduce the susceptible individuals. R_t does not reach zero, as in the previous surges, but remains constant at some equilibria of $R_t < 1$. Therefore, there is still ongoing transmission. However, the situation tends to decrease to a controllable level in early October 2021. This supports the effectiveness of the strict lockdown measure. Despite a few further transmissions and new cases, the outbreak is under control eventually. Whereas reaching zero rapidly for the estimated R_t corresponding to the convergence to the final size too early of the DNN and SNN models indicates the outbreak terminated in short. So, these models track the future trend in the wrong direction.

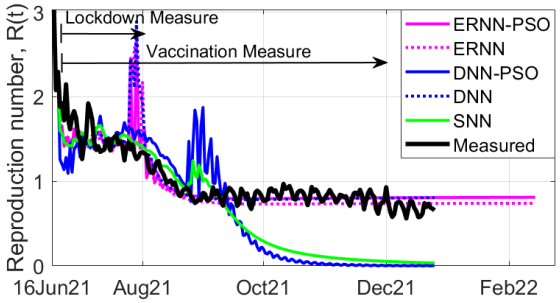

Figure 19. Reproduction number (Rt) obtained from ERNN, DNN, and SNN models with the measured data under lockdown measure of the fourth surge COVID-19 in Thailand.

E. Fifth surge of Thailand's COVID-19 with the Omicron Variant (December 2021- June 2022)

In early December 2021, many visitors infected with the Omicron variant of COVID-19 has entered Thailand. The epidemic is becoming increasingly worrying, with the number of daily infections setting a record. As a result, 3,111,857 cases and 23,512 deaths have been reported. To project the cumulative number of infected cases in this surge, the past four surges of outbreak data are included in the training dataset. The performance of training ERNN model using these data in combination with some at the beginning of the fifth surge, is well performed (Figure 20). However, the predicted results are not as expected, resulting in large errors in the middle of this surge (Figure 21). This is due to the evolution of disease transmission that emerged from the different infection characteristics of each surge.

Since the daily infected cases of countries that have severely experienced the Omicron variant, such as South Africa, Nigeria, and the USA, are likely to follow a normal distribution (Figure 22), those in Thailand are expected to have a similar distribution, making predictions simple and more accurate. So, the outbreak data of these countries, along with those of the previous three surges of Thailand, are included in the training dataset to improve the performance of the prediction models. With this new training dataset, the models could be trained well (Figure 23).

In the test, the proposed ERNN-PSO outperforms the rest in terms of a low error in estimating the final epidemic size, low RMSE and high reliability with a higher correlation coefficient and model-fit with higher R^2 to characterize the developing trends (Figure 24 and Table 7).

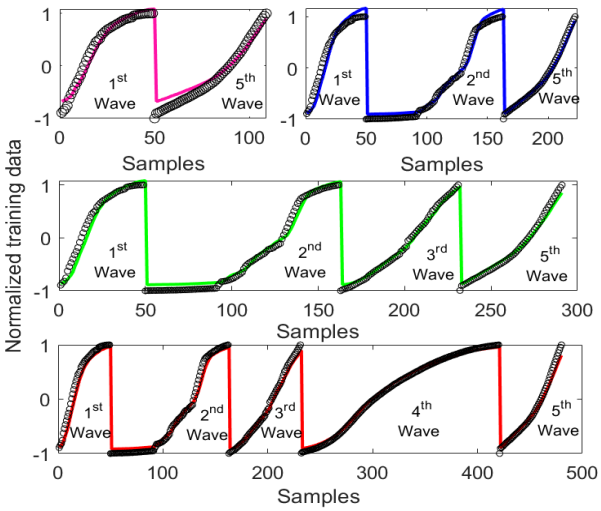

Figure 20. Training the ERNN model using the outbreak data from Thailand's previous four surges in combinations for Thailand's fifth surge of the COVID-19 epidemic.

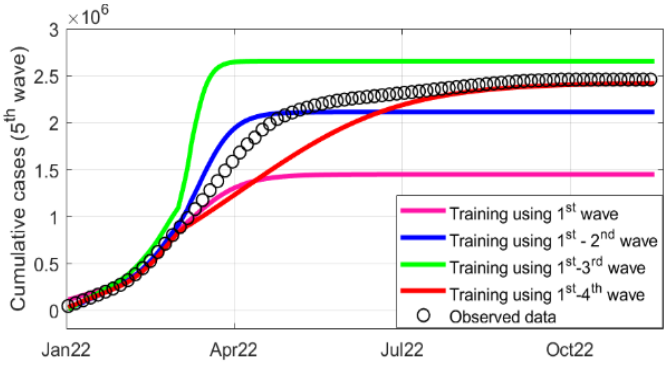

Figure 21. Prediction results of the proposed ERNN model using the outbreak data in combination with Thailand's previous four surges in training for Thailand's fifth surge of COVID-19 epidemic.

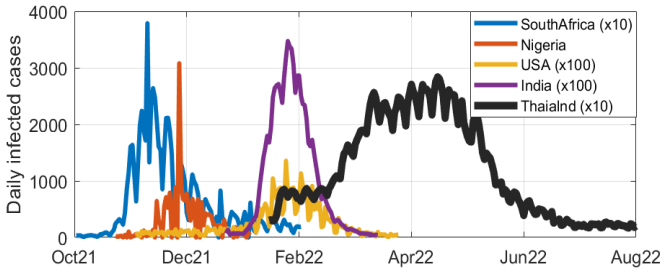

Figure 22. The distribution of the daily infected cases in some countries experienced the Omicron variant compared to those of Thailand's fifth surge of the COVID-19 epidemic.

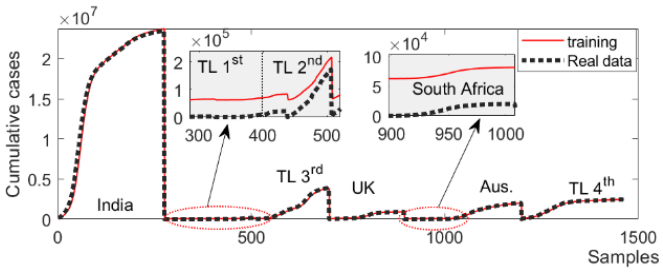

Figure 23. Training performance of the ERNN model using the outbreak data in combination with India, the UK, Australia, and Thailand's previous four surges to predict the fifth surge of the COVID-19 epidemic in Thailand.

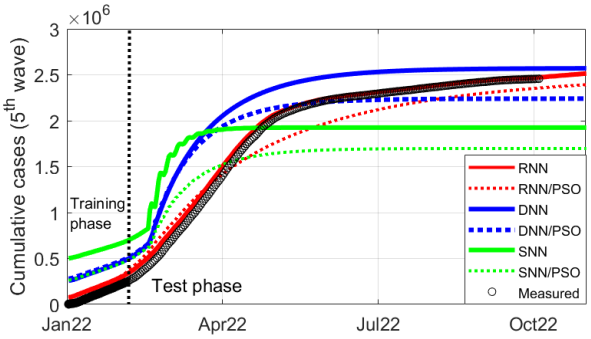

Figure 24. The prediction results of cumulative cases of the proposed models using the outbreak data in combination with the previous four surges of Thailand and those from India, UK, SA, and Aus. in training for Thailand's fifth surge of COVID-19 epidemic.

Models	Final epidemic size		Developing trends		
	Forecast	Error*	RMSE	ρ	R^2
RNN-PSO	2.52×10^6	1.52×10^4	1.36×10^4	0.999	0.97
RNN	2.34×10^6	1.10×10^5	1.89×10^5	0.997	0.95
DNN-PSO	2.55×10^6	1.78×10^5	3.54×10^5	0.979	0.96
DNN	2.20×10^6	2.53×10^5	4.94×10^6	0.963	0.93
SNN-PSO	1.82×10^6	6.32×10^5	4.8×10^5	0.952	0.91
SNN	1.64×10^6	8.12×10^5	5.08×10^5	0.944	0.91

Table 7. Comparative analysis of prediction models for Thailand's fifth surge of COVID-19, with the actual final epidemic size recorded as 2,456,727*.

The estimated R_t values obtained from the ERNN-PSO and ERNN models are consistent with the measured data (Figure 25). The R_t declines over time due to full vaccines across the country applied in this surge. However, the re-infection with the new virus mutant or inefficacy of the vaccines causes R_t to reach not to zero but at some equilibria of $R_t < 1$. Therefore, the outbreak continues under controlled conditions.

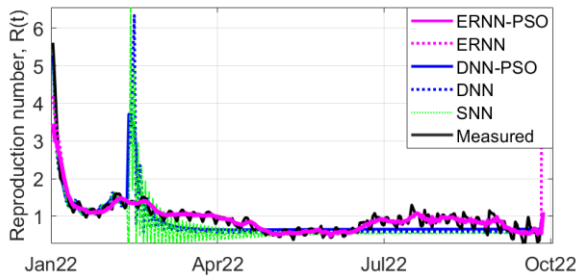

Figure 25. Reproduction number (R_t) obtained from ERNN, DNN, and SNN models with the measured data under lockdown measure of fifth surge COVID-19 in Thailand.

IV. Conclusion

For this study, the COVID-19 prediction models based on DNN and ERNN, are proposed to estimate the final epidemic size and characterize the cumulative cases. The PSO helps to improve their performance. When implemented in the first to fifth surges of COVID-19 in Thailand, the ERNN-PSO outperforms the rest in terms of accuracy and reliability. This supports the advantage of a NN model-based memory units. For the direction of improvement, the exogenous time series affecting the outbreak are incorporated into the predictor set. Moreover, other types of RNNs can be used to implement a more efficient predictive model.

References

[1] A. Zeb, E. Alzahrani, V.S. Erturk, G. Zaman. "Mathematical model for coronavirus disease 2019 (COVID-19) containing isolation class," *BioMed Research International*, pp. 1-7, 2020.

[2] J.K. Ghosh, S.K. Siswas, S. Sarkar, U. Ghosh. "Mathematical modelling of COVID-19: A case study of Italy," *Mathematics and Computers in Simulation*, 194, pp. 1-18, 2022.

[3] S.K. Yadav, Y. Akhter. "Statistical modeling for the prediction of infectious disease dissemination with special reference to COVID-19 spread," *Frontiers in Public Health*, 9, pp. 1-27, 2021.

[4] N.P. Jewell. "Statistical models for COVID-19 incidence, cumulative prevalence, and R_t," *Journal of the American Statistical Association*, 116(536), pp. 1578-582, 2021.

[5] R. Wongsathan. "The logistic growth regression model with the genetic algorithm for predicting the third surge of the COVID-19 epidemic in Thailand" *Asia-Pacific Journal of Science and Technology*, 28(1), pp. 1-16, 2023.

[6] R. Kafieh, R. Arian, N. Saeedizadh, Z. Amini, N.D. Sere, S. Minaee, et al. "COVID-19 in Iran: forecasting pandemic using deep learning," *Computational and Mathematical Methods in Medicine*, pp. 1-16, 2021.

[7] M. Wieczorek, J. Siłka, D. Połap, M. Woźniak, R. Damasˇevičius. "Real-time neural network based predictor for cov19 virus spread," *PLoS ONE*, 15(12), pp. 1-18, 2020.

[8] H.R. Niazkar, M. Niazkar. "Application of artificial neural networks to predict the COVID-19 outbreak," *Global Health Research and Policy*, 5(50), pp. 1-11, 2020.

[9] A. Alamsyah, B. Prasetiyo, M.F.A. Hakim, F.F. Pradana. "Prediction of COVID-19 using recurrent neural network model," *Scientific Journal of Informatics*, 8(1), pp. 1-6, 2021.

[10] A. Priyanka, M.S. Kumari. "Implementation of simple RNN and LSTMs based prediction model for coronavirus disease (COVID-19)," *IOP Conference Series: Materials Science and Engineering*, 1022, pp. 1-10, 2021.

[11] M. Alazab, A. Awajan, A. Mesleh, A. Abraham, V. Jatana. "COVID-19 prediction and detection using deep learning," *International Journal of Computer Information Systems and Industrial Management Applications*, 12, pp. 168-181, 2020.

[12] Q. Li, R.C. Lin. "A new approach for chaotic time series prediction using recurrent neural network," *Mathematical Problem in Engineering*, pp. 1-9, 2016.

[13] F. Shahid, A. Zameer, M. Muneeb. "Predictions for COVID-19 with deep learning models of LSTM, GRU and Bi-LSTM," *Chaos Solitons Fractals*, 140, pp. 1-10, 2020.

[14] K.K.A Ghany, H.M. Zawbaa, H.M. Sabri. "COVID-19 prediction using LSTM algorithm: GCC case study," *Informatics in Medicine Unlocked*, 23, pp. 1-9, 2021.

[15] J.P. Sarkar, I. Saha, N. Ghosh, D. Maity, D. Plewczynski. "Online predictor using machine learning to predict novel coronavirus and other pathogenic viruses," *ACS Omega*, 7(27), pp. 23069-74, 2022.

[16] F.M. Al-Humaidan, P.P. Rahoof, S.M. Sameer. "PSO and ABC based novel carrier frequency offset estimation techniques for Wi-MAX uplink transmission," *International Journal of Computer Information Systems and Industrial Management Applications*, 5, pp. 597-605, 2013.

[17] N.I. Anuar, M.H.F. Md Fauadi. A study on multi-objective particle swarm optimization in solving job-shop scheduling problem," *International Journal of Computer Information Systems and Industrial Management Applications*, 13, pp. 051-061, 2021.

[18] N. Srivastava, G. Hinton, A. Krizhevsky, I. Sutskever, R. Salakhutdinov. "Dropout: A simple way to prevent neural networks from overfitting," *Journal of Machine Learning Research*, 15, pp. 1929-58, 2014.

[19] J.L. Elman. "Finding Structure in Time," *Cognitive Science*, 14(2), pp. 179-211, 1990.

[20] L. Rosero-Bixby, T. Miller. "The mathematics of the reproduction number R for COVID-19: *A primer for demographers*, *Vienna Yearbook of Population Research*, 20, pp. 143-166, 2022.

[21] R. Wongsathan. "Real-Time prediction of the COVID-19 epidemic in Thailand using simple model-free method and time series regression model," *Walailak Journal of Science and Technology*, 18(14), pp. 1-11, 2021.

Author Biographies

Rati Wongsathan was born in Lamphun, Thailand. He received his B.Eng. (Hons.) Electrical Engineering, M. Eng. Electrical Engineering, M.Sc. Applied Mathematics from Chiang Mai University (CMU), Chiang Mai, Thailand in 1997, 2000, and 2005, respectively, and PhD Electrical Engineering from King Mongkut's Institute of Technology Ladkrabang (KMITL), Bangkok, Thailand in 2020. His research interests are in the areas of renewable energy, mathematical model, telecommunications, data storage, optimization, AI, and engineering education. He has published over 30 journal articles with impact factors, 20 conference papers, and 2 books. He currently served as an assistant professor at Faculty of Engineering and Technology of North-Chiang Mai University (NCU), Chiang Mai, Thailand.

Wutthichai Puangmanee was born in Lampang, Thailand. He received his B. Ed. Computer Education from Lampang Rajabhat University, Thailand in 2004, the M.Sc. Internet and Information Technology from Naresuan University, Phitsanulok, Thailand in 2007. He is currently pursuing a PhD in Computer Engineering, Kasetsart University, Bangkok, Thailand. His research interests are embedded systems, automation systems, and machine learning.